Pablo Jahir Peña-Obeso, Rafael Huirache-Acuña*, Manuel Arroyo-Albiter, Santiago José Guevara-Martínez, Carolina Leyva and Maritza E. Cervantes-Gaxiola*

Hydrodesulfurization of dibenzothiophene using NiMoWS catalysts supported on Al–Mg and Ti–Mg mixed oxides

https://doi.org/10.1515/ijcre-2019-0216
Received November 29, 2019; accepted June 23, 2020; published online July 31, 2020

Abstract: In this work, two series of trimetallic NiMoW sulfide catalysts supported on Al–Mg(x) and Ti–Mg(x) mixed oxides with different content of MgO (x = 5, 10, 15 and 20 wt.% of MgO) were synthesized. The mixed oxides and catalysts were characterized by X-ray diffraction (XRD), Fourier-transform infrared (FT-IR) spectroscopy, N_2 physisorption and Diffuse reflectance spectroscopy (DRS UV–Vis); and evaluated during the hydrodesulfurization (HDS) of dibenzothiophene (DBT) reaction. The NiMoW/Al–Mg catalysts showed a higher dispersion of Ni, Mo and W species than NiMoW/Ti–Mg catalysts resulting in higher catalytic activities. Catalysts with 10 wt.% of MgO showed the highest catalytic activity for both series of catalysts. Most of the synthesized catalysts exhibited higher activities than NiMoWS/Al–Ti reference catalyst. The present comparison study clearly showed that NiMoW/Al–Mg and NiMoW/Ti–Mg catalyst with 10 wt.% of MgO might be a promising and effective catalyst for the HDS-DBT reaction.

Keywords: Al–Mg(x); dibenzothiophene; hydrodesulfurization; NiMoW; Ti–Mg(x).

***Corresponding authors: Rafael Huirache-Acuña**, Facultad de Ingeniería Química, Universidad Michoacana de San Nicolás de Hidalgo, Ciudad Universitaria, Morelia, 58030, Michoacán, Mexico, E-mail: rafael_huirache@yahoo.it; and **Maritza E. Cervantes-Gaxiola**, Facultad de Ciencias Químico Biológicas, Universidad Autónoma de Sinaloa, Culiacan, 80030, Sinaloa, Mexico, E-mail: mecg@uas.edu.mx
Pablo Jahir Peña-Obeso: Facultad de Ciencias Químico Biológicas, Universidad Autónoma de Sinaloa, Culiacan, 80030, Sinaloa, Mexico; Facultad de Ingeniería Química, Universidad Michoacana de San Nicolás de Hidalgo, Ciudad Universitaria, Morelia, 58030, Michoacán, Mexico
Manuel Arroyo-Albiter and Santiago José Guevara-Martínez: Instituto de Investigaciones Químico-Biológicas, Universidad Michoacana de San Nicolás de Hidalgo, Morelia, 58030, Michoacán, Mexico
Carolina Leyva: Instituto Politécnico Nacional, CICATA Unidad Legaria, Legaria 694, Irrigación, Mexico City, 11500, Mexico

1 Introduction

Since the United States Environmental Protection Agency (EPA) in 2006 gradually began to apply stricter regulations to reduce the amount of sulfur in diesel fuel to 15 ppm, known as ultra-low sulfur diesel (ULSD) (EPA 2006), the global tendency in ULSD diesel is to reduce the sulfur concentration of 10 ppm or even lower to prevent air contamination in crowded cities (Díaz de León et al. 2019). In combination with cleaner-burning diesel engines and vehicles, ULSD fuel will help to improve air quality by significantly reducing emissions (API 2020). Hydrodesulfurization (HDS) is the most common process used in the petroleum industry to reduce the sulfur content of fuel products. Traditionally, MoS_2 and WS_2 supported on alumina and promoted by Co or Ni are used as catalysts in the HDS process (Girgis and Gates 1991). However, to achieve the ULSD, it is necessary to remove total sulfur from refractory compounds like dibenzothiophene (DBT) and its derivatives that are present in the diesel feeds (Rana et al. 2018). In this sense, the modification of traditional catalysts or even new formulations is required. Active metal dispersion over support, metal-support interaction, active phases, morphology, and catalyst stability are some of the most important factors in the design of HDS catalysts (Chianelli and Berhault 1999; Chianelli et al. 1995; Costa et al. 2004; Cruz-Perez et al. 2011; Dufresne et al. 1996; Harris and Chianelli 1984; Kelty, Berhault, and Chianelli 2007; Leyva et al. 2012; Portela, Grange, and Delmon 1995; Scheffer et al. 1990; Topsøe 2007; Topsøe and Clausen 1984; Vangestel, Leglise, and Duchet 1994; Vrinat et al. 1994). With this in mind, an unsupported NiMoW sulfide catalyst was synthesized and patented, which exhibited to be until three times more active than traditionally used catalysts (Soled et al. 2001). However, the low surface area, sintering of catalysts, the high cost and low dispersion of active phases represent challenges for the industrial use of trimetallic catalysts.

In particular, the support plays an important role in the dispersion of active species and affects the metal-support

interactions (Absi-Halabi, Stanislaus, and Al-Dolama 1998; Okamoto et al. 2003; Ríos-Caloch et al. 2016). The above has motivated the research of materials with the adequate properties to be used as supports for trimetallic NiMoWS catalysts, among them are Al_2O_3 (González-Cortés et al. 2014; Lan et al. 2011; Mozhaev et al. 2018; Nikulshina et al. 2017; Sigurdson, Sundaramurthy, and Dalai 2008), AAS–Al_2O_3 (Dik et al. 2018), SBA-15 (Mendoza-Nieto et al. 2013), Ti-SBA-15 and Zr-SBA-15 (Mendoza-Nieto et al. 2019), TiO_2-SBA-15 (Gómez-Orozco et al. 2018), Al_2O_3–TiO_2 (Cervantes-Gaxiola et al. 2012), Al_2O_3–TiO_2–MgO (Cervantes-Gaxiola et al. 2012), P-containing SBA-16 (Guzmán et al. 2013), Al-HMS and Al-SBA-16 (Huirache-Acuña et al. 2012); and HMS-Ti (Vázquez-Salas et al. 2018).

It is important to highlight that significant efforts have been developed to understand the structure-activity correlations in HDS catalysts (Chianelli et al. 2002; Göbölös et al. 1986; Harris and Chianelli 1984; Knudsen, Cooper, and Topsøe 1999; Okamoto 2014; Ramírez and Gutiérrez-Alejandre 1998; Topsøe and Clausen 1984; van Haandel et al. 2015). Nevertheless, Díaz de León et al. (2019) point out that the exact composition of each support participating in the new mixed oxide always plays a role in the final observed catalytic properties.

Particularly, the use of Al_2O_3–TiO_2 mixed oxide as supports for HDS catalysts reported that the presence of TiO_2 facilitates the reduction and sulfidation of Mo and W active phases, which leads to the formation of octahedral type sites of Mo oxide species (Grzechowiak, Rynkowski, and Wereszczako-Zieliñska 2001). These octahedral Mo oxide species unlike the tetrahedral ones interact weakly with the supports and as a consequence are easily reduced and sulfided resulting in higher activity in HDS reactions.

Furthermore, MgO on mixed oxides to be used as support for HDS catalysts have also been proposed because it can improve surface properties, such as the generation of acid–base sites and support basicity (Klicpera and Zdražil 1999, 2002; Solis et al. 2004). Also, MgO properties can favor interactions between support and acid species of Mo, which increases the formation of highly dispersed species in CoMoS and NiMoS catalysts, and also inhibit the formation of coke, which is common in MoS_2 and NiMoS catalysts supported on Al_2O_3 (Klimova, Solís Casados, and Ramírez 1998). However, MgO can react with air moisture to form a mixture of $Mg(OH)_2$ and $Mg(CO_3)_2$ when is it exposed during prolonged periods of time to ambient conditions or during aqueous impregnation (Solis et al. 2004).

On the other hand, the effect of the addition of MgO to alumina on the properties of catalysts for hydrotreatment reactions has been well documented. Grzechowiak, Rynkowski, and Wereszczako-Zieliñska (2001) studied the incorporation of small amounts of MgO in MoS_2 and NiMoS catalysts supported on Al_2O_3 and reported that MgO did not change the structure of Al_2O_3. Studies of catalysts supported on Al_2O_3–MgO reported an increase in specific surface area and mesoporous pore size distributions, which is necessary for hydrotreatment processes (Guevara-Lara et al. 2010; Klimova, Solís Casados, and Ramírez 1998; Mogica-Betancourt et al. 2014; Trejo, Rana, and Ancheyta 2008). Other studies of CoMoS/Al_2O_3–MgO catalysts showed an improvement in the dispersion of Co and Mo species with the increase of MgO content, these species were polymolybdate groups with Mo–O–Co bonds, and as a result, an increase in HDS activity was observed (Trejo, Rana, and Ancheyta 2008; Wu et al. 2009). However, reports in HDS activity using Al_2O_3–MgO as a support are controversial. NiMo/Al_2O_3–MgO catalysts have shown lower HDS activity with the addition of MgO content due to the formation of NiO–MgO species that reduce the effects of Ni promoter (Klimova, Solís Casados, and Ramírez 1998). However, high HDS activities were reported for NiMo/Al_2O_3–MgO due to the formation of Ni^{+2} species interacting with MoO_4^{+2} and $Mo_7O_{24}^{-6}$ (Guevara-Lara et al. 2010). Mogica-Betancourt et al. (2014) reported easier sulfidation of W species with the addition of 5 wt.% of MgO on NiW/Al_2O_3–MgO catalysts. Besides, the NiMo/Al_2O_3–MgO catalyst was more resistant to quinoline inhibition in the competitive HDS-hydrodenitrogenation reactions than NiMo/Al_2O_3 and NiMo/Al_2O_3–TiO_2 (Vázquez-Garrido et al. 2019). Finally, in another study the Mg considered as an impurity in the Al_2O_3 produced better performance in the supported NiMo catalysts during the HDS of DBT reaction, attributed to the fact that the Mg change the nature of the active phase and support surface interaction, promoting a greater dispersion of Mo species (Romero-Toledo et al. 2018).

Nevertheless, the use of TiO_2–MgO mixed oxide has been less reported. Particularly, Cruz-Pérez et al. (2016) reported that NiWS/TiO_2–MgO HDS catalysts with higher surface areas, the abscence of NiO and $NiWO_4$ species, higher dispersion of Ni and W species and the presence of W in an octahedral symmetry and Ni in tetrahedral symmetry. Besides, the use of TiO_2–MgO also decreased the interaction between metal-support and increased HDS catalyst activity. Finally, some studies reported more complex formulations using MgO, for instance NiMoWS/Al–Ti–Mg (Cervantes-Gaxiola et al. 2012, 2013), CoMo/

Al_2O_3–MgO–Li (Solís-Casados et al. 2016) and CoMoW/Al_2O_3–MgO–K_2O (Solís-Casados et al. 2019).

In our previous work, NiMoWS/Al_2O_3–TiO_2–MgO catalysts with small wt.% of MgO showed better structural, superficial, textural and catalytic properties during the HDS-DBT than NiMoWS/Al_2O_3–TiO_2 (Cervantes-Gaxiola et al. 2012). In literature, the study of catalysts based on NiMoW sulfides supported on Al_2O_3–MgO and TiO_2–MgO has not been reported to date. Because of this, the purpose of this investigation is focused on the comparative study of catalytic properties of NiMoW/Al–Mg and NiMoW/Ti–Mg with different wt.% of MgO and their performance during the HDS of DBT reaction.

2 Experimental

2.1 Synthesis of Al_2O_3–MgO and TiO_2–MgO supports

Based on the procedure reported by Cervantes-Gaxiola et al. (2012), the Al_2O_3–MgO(x) TiO_2–MgO(x) mixed oxides were synthesized by the sol-gel method, using x = 5, 10, 15 and 20 wt.% of MgO. The required amount of aluminum-tri-sec-butoxide ($Al(OC_4H_9)_3$) or titanium-butoxide ($Ti(OC_4H_9)_4$) were added to 150 ml of isopropanol at 60 °C and kept stirred for 1 h. Later, the solution was cooled down at 3 °C. Separately, a hydrolysis solution was prepared using deionized water, ethanol, isopropanol and nitric acid (13:8:5:0.5 ml) in which the adequate amount of magnesium nitrate hexahydrate ($Mg(NO_3)_2{\cdot}6H_2O$) was dissolved. This solution was added dropwise to the alkoxide solution to obtain a gel. The gel was aged at low temperature for 24 h and then dried at room temperature. Finally, the solids obtained were calcined under air flow at 500 °C for 4 h (heating rate of 10 °C/min). The mixed oxides were labeled as follows: Al–Mg 05, 10, 15, 20 and Ti–Mg 05, 10, 15, 20; where Al = Al_2O_3, Mg = MgO, Ti = TiO_2, and the number represents wt.% of MgO.

2.2 Synthesis of NiMoW/Al–Mg and NiMoW/Ti–Mg sulfide catalysts

Trimetallic NiMoW sulfide catalysts were synthesized by the co-impregnation method using an atomic ratio of Ni/[Ni+(Mo+W)] = 0.5; and a molar ratio of Mo:W 1:1 (18 wt.%). Ammonium thiomolybdate (TMA) and ammonium thiotungstate (TTA), which were synthesized in the laboratory by previously reported methods (Krüss 1884; Ramanathan and Weller 1985; Vega-Granados et al. 2017), and nickel nitrate hexahydrate ($Ni(NO_3)_2{\cdot}6H_2O$) were used as precursors. The required amount of each precursor was dissolved separately in deionized water, and then the solutions of precursors were mixed to obtain a dark solution which was added to the support by impregnation in several steps. After each step, the support was dried at 120 °C for 2 h. The impregnated supports were then calcined at 450 °C (heating rate of 10 °C/min) for 4 h, and subsequently reduced and activated under a flow of H_2S/H_2 (15% v/v) at 400 °C (heating rate of 4 °C/min) for 4 h. Catalysts were labeled as follows: NiMoW/Al–Mg 05, 10, 15, 20; NiMoW/Ti–Mg, 05, 10, 15, and 20; where the number indicates the wt.% of MgO.

2.3 Characterization techniques

The structural characteristics of trimetallic NiMoW supported catalysts in their oxide and sulfide states were determined by X-ray diffraction (XRD) using a D8 Advance AXS Bruker diffractometer equipped with a CuK_α radiation under the following conditions: 2θ range 10°–85°, wavelength λ = 1.54 Å, operating voltage of 30 kV and a current of 30 mA.

Fourier-transform infrared (FT-IR) spectra were used to identify the surface functional groups on Al_2O_3–MgO and TiO_2–MgO supports using a Nicolet iS 10 FT-IR Spectrometer by the attenuated total reflectance (ATR) technique. The spectra were obtained at room temperature in the range of 4000–400 cm^{-1}, with four scans and 4 cm^{-1} of resolution. The background was taken before each sample analysis and no acid or basic sites were evaluated, only those of metal oxides.

The textural properties of Al_2O_3–MgO and TiO_2–MgO supports, NiMoW/Al–Mg and NiMoW/Ti–Mg sulfide catalysts were determined from the adsorption-desorption isotherms of nitrogen at –196 °C using a Quantachrome Novatouch Lx 1 analyzer. Before the analysis the samples were treated at 200 °C for 5 h under vacuum. The specific surface areas of the samples were calculated by the Brunauer, Emmett, and Teller (BET) method considering the relative pressure interval of $0.05 < P/P_0 < 0.3$. The pore size distributions were obtained by the Barret–Joyner–Halenda method (BJH).

The UV–vis diffuse reflectance spectra of NiMoW/Al–Mg and NiMoW/Ti–Mg catalysts in oxide state were recorded using a Varian Cary 100 Spectrophotometer equipped with an integrating sphere as a reference and calibrated using MgO in the 200–1000 nm interval. During

the recording of the reflectance data, the Kubelka-Munk function was applied:

$$F(R_\infty) = \frac{(1 - R_\infty)^2}{2R_\infty} \quad (1)$$

here R_∞ is the reflectance at infinite depth.

2.4 Catalytic activity measurements

Trimetallic NiMoW/Al–Mg and NiMoW/Ti–Mg sulfide catalysts were evaluated in the hydrodesulfurization of the dibenzothiophene reaction (HDS-DBT). The tests were carried out in a high-pressure Parr 4560 batch reactor in which 75 mL of a solution of DBT and n-heptane (5 vol.% of DBT in n-heptane); and 0.5 g of the corresponding trimetallic catalyst were added. The reactor was pressurized at 3.1 MPa using hydrogen and then was gradually heated until to reach the reaction temperature of 350 °C, using a stirring rate of 600 rpm. Reaction time was 5 h and liquid samples were collected every half an hour. Liquid samples were analyzed with a 4890 model Hewlett Packard gas chromatograph equipped with flame ionization (FID) detector and an HP-Ultra 2 column (30 m × 0.32 mm id.). Catalytic activity was investigated in terms of DBT conversion, a pseudo-zero-order reaction-rate constant (k), and the selectivity after 5 h when the conversion reached a steady state. From data on DBT conversion as a function of time, the reaction rate constant was calculated by the equation (Candia, Clausen, and Topsøe 1982; Huang et al. 2008):

$$x_{DBT} = \frac{1 - n_{DBT}}{n_{DBT}} = \frac{k}{n_{DBT,0}} t \quad (2)$$

where: x_{DBT} is the conversion fraction of DBT, n_{DBT} is the moles of DBT (mol), k is the pseudo-zero order reaction-rate constant (mol s^{-1} g^{-1}), t is the time in seconds (s) and $k/n_{DBT,0}$ is the slope.

According to Houalla et al. (1980), the HDS-DBT reaction yields two different products: biphenyl (BP) is produced through direct desulfurization (DDS) pathway and cyclohexylbenzene is produced through hydrogenation (HYD) pathway. Since these two pathways are parallel, the selectivity was calculated using the following equation:

$$\frac{HYD}{DDS} = \frac{[THDBT] + [CHB]}{[BP]} \quad (3)$$

For comparative purposes, a NiMoW/Al–Ti (20 wt.% of TiO_2) catalyst was used as a reference.

3 Results and discussion

3.1 X-ray diffraction (XRD)

The XRD patterns of Al–Mg and Ti–Mg mixed oxide supports are shown in Figure 1. The XRD patterns of Al–Mg mixed oxides (Figure 1A) only show two broad and low intense peaks at 2θ = 37.36° and 46.26° corresponding to γ-Al_2O_3 (JCPDS No. 046-1212). All Al–Mg supports have similar diffraction patterns regardless the MgO content, which indicates a good dispersion of MgO on the surface of

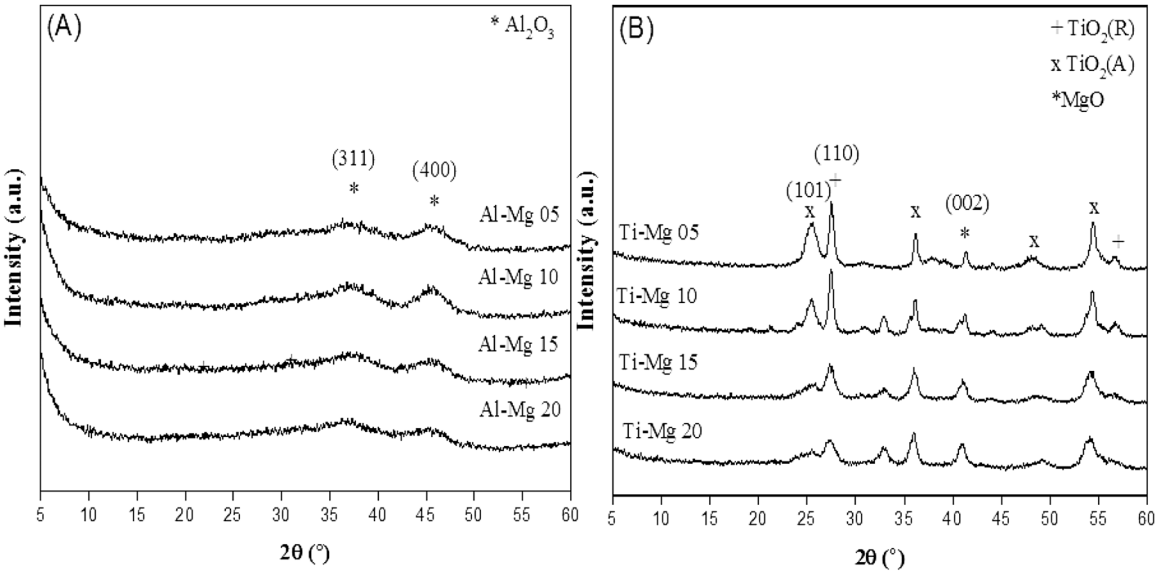

Figure 1: XRD patterns of (A) Al–Mg and (B) Ti–Mg mixed oxides.

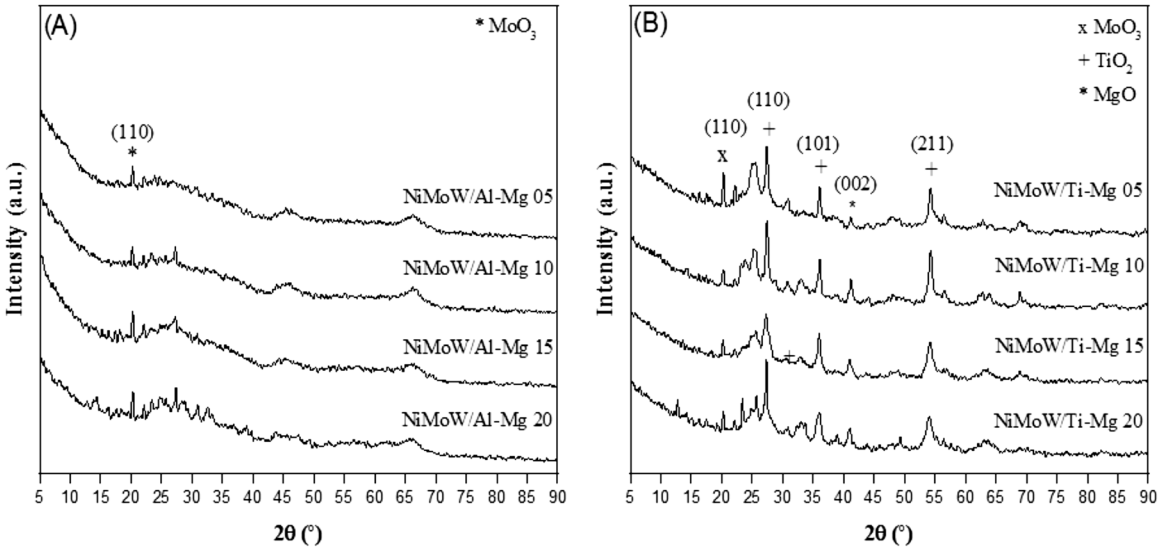

Figure 2: XRD patterns of (A) NiMoW/Al–Mg and (B) NiMoW/Ti–Mg catalysts in the oxide state.

the γ-Al_2O_3. These results reveal that γ-Al_2O_3 is the main crystalline structure and the addition of up to 20 wt.% of MgO does not affect the alumina structure and also maintains it, which is in agreement with previous results (Grzechowiak, Rynkowski, and Wereszczako-Zieliñska 2001). The low intensity of XRD peaks indicates that Al–Mg mixed oxides are amorphous materials.

On the other hand, the diffraction patterns of Ti–Mg mixed oxides (Figure 1B) show well-defined peaks corresponding to a phase mixture of anatase and rutile peaks at 2θ = 26.66°, 38.96° and 56.53° assigned to TiO_2 anatase (JCPDS No. 004-0477); and peaks at 2θ = 27.52° and 32.88° corresponding to TiO_2 rutile phase (JCPDS No. 004-0551). Also, it was observed one peak approximately at 2θ = 41.42° of MgO periclase (JCPDS No. 043-1022). Some differences are observed in the diffraction patterns, since when the MgO content increases the TiO_2 signals decrease.

Figure 2 shows the XRD patterns of NiMoW/Al–Mg and NiMoW/Ti–Mg catalysts in the oxide state. In Figure 2A all NiMoW/Al–Mg catalysts exhibit similar XRD patterns with poorly crystalline structures due to the low-intensity peaks at 2θ = 12.82°, 20.29°, 24.77°, 27.41° and 2θ = 45.49°, 66.67°, assigned to crystalline phases of MoO_3 (JCPDS No. 76-1003) and γ-Al_2O_3 (JCPDS No. 046-1212) (Priecel et al. 2011),

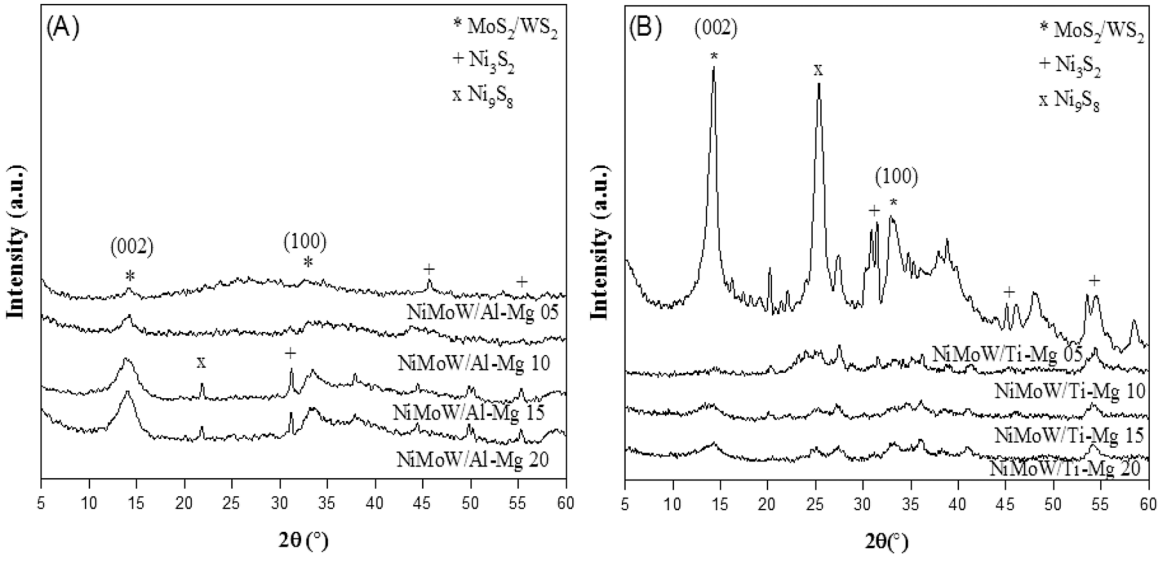

Figure 3: XRD patterns of (A) NiMoW/Al–Mg and (B) NiMoW/Ti–Mg sulfide catalysts.

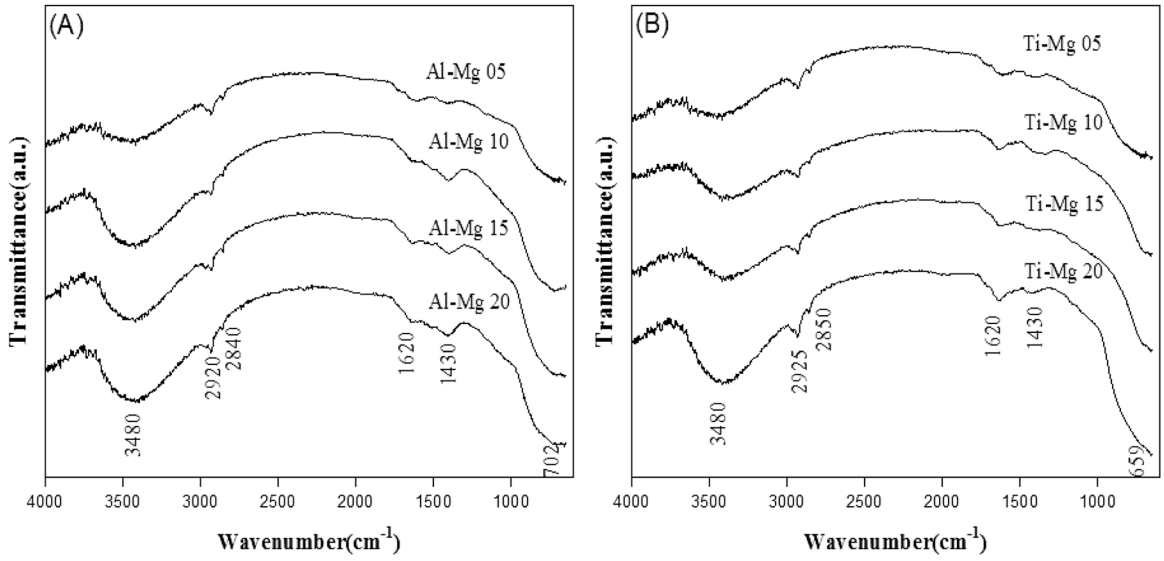

Figure 4: FT-IR spectra of (A) Al–Mg and (B) Ti–Mg mixed oxides.

respectively. It is possible to observe that with the addition of MgO the MoO_3 peaks are more intense. Besides, the XRD patterns did not detect obvious peaks of crystalline phases of NiO, WO_3, or $NiWO_4$. These results suggest a good dispersion of the metal oxide species present in the NiMoW catalysts supported on Al–Mg mixed oxides. On the other hand, Figure 2B shows the XRD patterns of NiMoW/Ti–Mg catalysts, where the characteristic peaks of MoO_3, MgO periclase and TiO_2 anatase phase are observed. The intensity of peaks assigned to MoO_3 decreases with the increasing of MgO content, an opposite effect was observed on the NiMoW/Al–Mg oxide catalysts. Similar effects of MgO loading on Al_2O_3 (Caloch, Rana, and Ancheyta 2004; Cervantes-Gaxiola et al. 2013; Klimova, Solís Casados, and Ramírez 1998; Rana et al. 2005) and TiO_2 (Cruz Pérez et al. 2016) were observed previously. From the comparison of diffraction patterns of NiMoW/Al–Mg and NiMoW/Ti–Mg catalysts it is possible to conclude that the latter presents more defined diffraction peaks due to the more crystalline structure.

Figure 3 shows the XRD patterns of NiMoW/Al–Mg and NiMoW/Ti–Mg in their sulfide state. First, in Figure 3A it is possible to observe NiMoW/Al–Mg sulfide catalysts with poorly crystalline structures due to low intense peaks at 2θ = 14.04° and 33.42°, which indicates the presence of MoS_2 and WS_2 phases (JCPDS No. 37-1492) (Cervantes-Gaxiola et al. 2013; Huirache-Acuña et al. 2006) in (002) and (100) planes, respectively. In particular, the (002) plane is characteristic of stacking in the "c" direction in the hexagonal cell. Besides, four more low intense peaks were detected at 2θ = 21.82° and 2θ = 31.14°, 44.46°, 55.34° corresponding to Ni_9S_8 (JCPDS No. 78-1886) and Ni_3S_2 (JCPDS No. 44-1418) phases (Nava, Pedraza, and Alonso 2005). The intensity of those peaks depends on wt.% of MgO, since more intense peaks are observed in the XRD patterns of NiMoW/Al–Mg 15 and NiMoW/Al–Mg 20 compared to the patterns of NiMoW/Al–Mg 5 and NiMoW/Al–Mg 10 sulfide catalysts. The low intensity of peaks of NiMoWS/Al–Mg 5 and NiMoWS/Al–Mg 10 indicates that most of the species should be widely dispersed on the Al–Mg supports. Regarding the NiMoW/Ti–Mg sulfide catalysts, in Figure 3B is observed the characteristic peaks of MoS_2, WS_2, Ni_3S_2 and Ni_9S_8 phases. However, in these catalysts the intensity of peaks decreases with the increase of the content of MgO.

3.2 FT-IR spectroscopy

In Figure 4 the FT-IR spectra of Al–Mg and Ti–Mg mixed oxide supports are compared. It is well known that H_2O and CO_2 molecules are easily chemisorbed onto the MgO surface when exposed to the environmental conditions. In this sense, all the spectra show bands at 3468 cm^{-1} and 1628 cm^{-1} corresponding to OH vibrations (stretching and bending, respectively) due to the surface-adsorbed water molecules (Ansari et al. 2017) and with the increasing of wt.% of MgO these bands become more intense. The bands around 2850 cm^{-1} and 2920 cm^{-1} are attributed to organic residues due to the reagents used in the reaction (alkoxides) and to the alcohol used as the solvent. Besides, the band at 1434 cm^{-1} is assigned to the presence of ionic CO_3^{-2} carbonate (Klimova, Solís Casados, and Ramírez 1998). Particularly, in Figure 4A one broad band in the region of

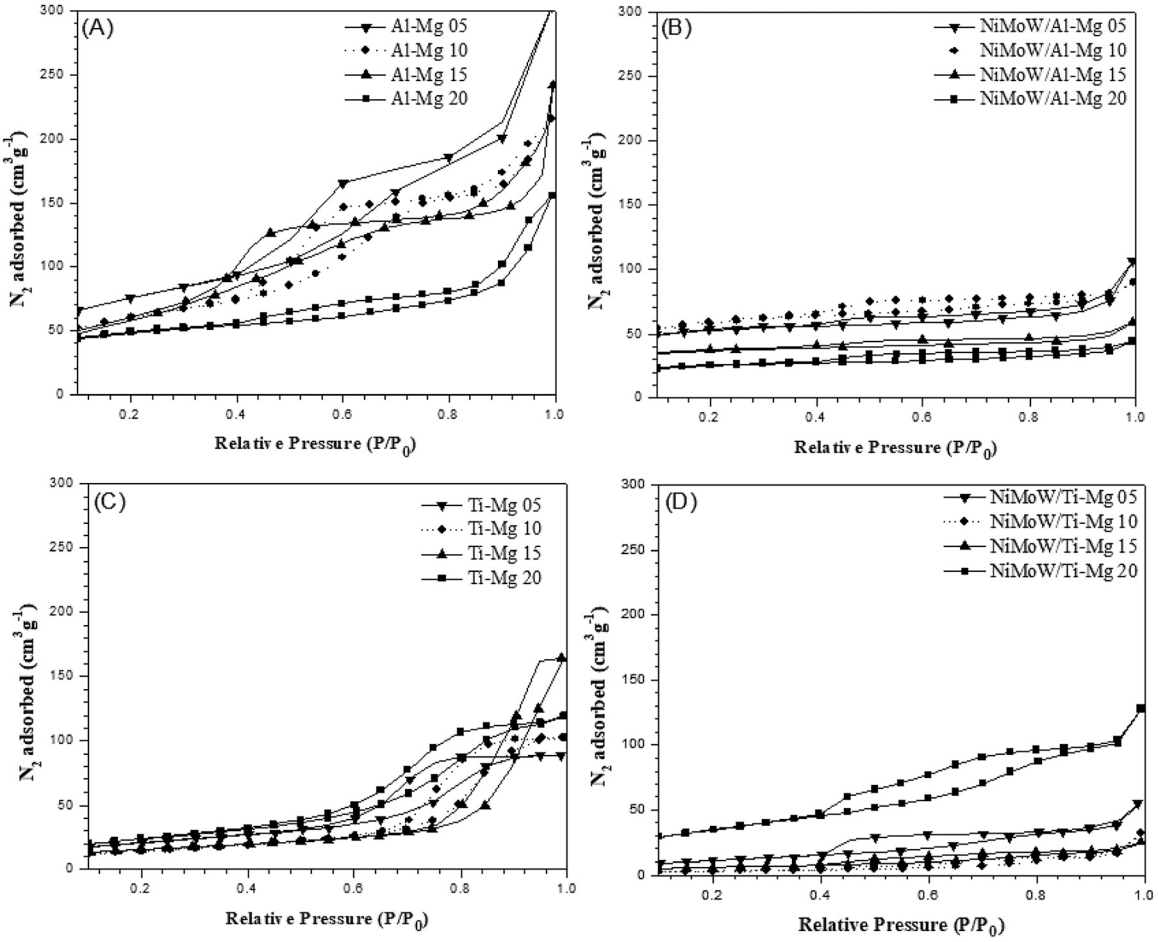

Figure 5: N_2 adsorption-desorption isotherms of (A) Al–Mg mixed oxides, (B) NiMoW/Al–Mg sulfide catalysts, (C) Ti–Mg mixed oxides and (D) NiMoW/Ti–Mg sulfide catalysts.

500–900 cm^{-1} is observed, which is related to Mg–O, Al–O and Mg–O–Al bonds (Sajjadi, Haghighi, and Rahmani 2015). On the other hand, in Figure 4B, the broad band in the range of 600–1000 cm^{-1} is attributed to the M-O-M vibration of Ti–Mg mixed oxides since it has been reported that Ti–O–Ti vibration bonds are formed within the range of 800–1000 cm^{-1}, whereas the main stretching bond of Mg–O is observed below 700 cm^{-1} (El-Sayed et al. 2018). These results indicate that the presence of surface-adsorbed water increases with the addition of MgO in agreement with previous works (Klimova, Solís Casados, and Ramírez 1998; Wu et al. 2009), however, this effect is more apparent in Al–Mg than Ti–Mg mixed oxides.

3.3 Nitrogen physisorption

The nitrogen adsorption-desorption isotherms of Al–Mg and Ti–Mg mixed oxides; trimetallic NiMoW/Al–Mg and NiMoW/Ti–Mg sulfide catalysts are shown in Figure 5. Both series of supports (Figure 5A and C) showed typical type IV adsorption isotherms (IUPAC classification) characteristic of mesoporous materials. Although it is observed that both series show an H2-type hysteresis loop, meaning that these supports have bottleneck shaped pores. Hysteresis loops of Al–Mg mixed oxides are extended, indicating high surface areas, while Ti–Mg supports showed broader hysteresis loops, suggesting a bigger pore volume than that of the Al–Mg supports. Also, it can be noted that the volume of N_2 adsorbed decreases with the increasing addition of MgO, which suggests pore occlusion in supports with at high MgO loading for Al–Mg supports, while the opposite effect can be seen on Ti–Mg supports. A similar trend can be found in the sulfide catalysts in Figure 5B and Figure 5D with the exception of NiMoWS/Ti–Mg 05. However, after the incorporation of the promoter and active phases, a drastic decrease of nitrogen adsorbed is observed in all sulfide catalysts.

The main textural properties for supports and sulfide catalysts are summarized in Table 1. Some differences in

Table 1: Specific surface area (S_{BET}) and average pore size (APS) of Al–Mg and Ti–Mg mixed oxides; trimetallic NiMoW/Al–Mg and NiMoW/Ti–Mg sulfide catalysts.

Support	S_{BET} (m^2/g)	APS (nm)	Sulfide catalysts	S_{BET} (m^2/g)	APS (nm)
Al–Mg 05	230.2	4.6	NiMoWS/Al–Mg 05	31.9	3.4
Al–Mg 10	218.9	4.3	NiMoWS/Al–Mg 10	40.5	3.4
Al–Mg 15	217.7	3.3	NiMoWS/Al–Mg 15	20.4	3.7
Al–Mg 20	69.7	3.4	NiMoWS/Al–Mg 20	25.0	3.8
Ti–Mg 05	82.7	6.7	NiMoWS/Ti–Mg 05	40.2	3.4
Ti–Mg 10	51.9	7.8	NiMoWS/Ti–Mg 10	19.6	3.4
Ti–Mg 15	80.2	12.0	NiMoWS/Ti–Mg 15	24.6	3.4
Ti–Mg 20	109.1	7.2	NiMoWS/Ti–Mg 20	130.6	3.4, 5.3

the specific surface area (S_{BET}) and average pore size (APS) can be found as a function of MgO loading for Al–Mg and Ti–Mg mixed oxides. For Al–Mg mixed oxide supports, there is a decreasing trend in S_{BET} and APS with the addition of MgO. However, the opposite effect is observed for Ti–Mg mixed oxides, where an increase in S_{BET} can be seen with the addition of MgO, with the exception of Ti–Mg 10, and the APS increases until 15 wt.% of MgO. In both series of supports a considerable drop in SSA is noticeable after the Ni, Mo, and W metals were deposited on supports. The significant reduction of SSA indicated that parts of pores of mixed oxides were blocked due to the impregnation method. However, in both series of catalysts, the SSA does not show a clear effect as a function of wt.% of MgO. Finally, APS of NiMoWS/Al–Mg and NiMoW/Ti–Mg sulfide catalysts are very similar (3.4–3.8 nm) independently of the wt.% of MgO.

The pore size distributions of Al–Mg and Ti–Mg mixed oxides are shown in Figure 6A and Figure 6C, respectively. All supports show a mesoporous nature. The Al–Mg mixed oxides exhibit the following pore size distributions: Al–Mg 5 (3–8 nm), Al–Mg 10 (3–7 nm), Al–Mg 15 (3–6 nm) and Al–Mg 20 (3–5 nm), and it is evident that with the increase of MgO content on Al-Mg the pore size distribution is narrower. However, an opposite effect is observed for Ti-Mg mixed oxides, which present the next pore size distribution: Ti–Mg 5 (3–12 nm), Ti–Mg 10 (4–18 nm), Ti–Mg 15 (6–50 nm) and Ti–Mg 20 (3–17 nm), apparently the pore size distribution is broader with the addition of MgO. The pore size distributions of NiMoW/Al–Mg and NiMoW/Ti–Mg sulfide catalysts are presented in Figure 6B and Figure 6D, respectively. It is important to note that a decrease in pore size distribution occurred after the deposition of the active phases and this effect is more evident on NiMoW/Ti–Mg sulfide catalysts. All NiMoW/Al–Mg catalysts exhibit similar pore size distribution (3–4.5 nm). While NiMoW/Ti–Mg catalysts have the following pore size: NiMoW/Ti–Mg 05 (3–8 nm), NiMoW/Ti–Mg 10 (3–8 nm), NiMoW/Ti–Mg 15 (3–8 nm) and NiMoW/Ti–Mg 20 (3–4 nm and 4–12 nm, bimodal distribution).

3.4 UV–vis diffuse reflectance spectroscopy

The UV–Vis diffuse reflectance (DRS) spectra of the trimetallic NiMoW/Al–Mg and NiMoW/Ti–Mg sulfide catalysts in the oxide state are shown in Figure 7. First, the NiMoW/Al–Mg spectra (Figure 7A) show one band at 241 nm, which is normally attributed to tetrahedral molybdate species, which indicates a good dispersion of Mo species (Duan et al. 2007), while the shoulder located at 272 nm observed in NiMoW/Al–Mg 5 catalyst spectra can be attributed to $Mo_7O_{24}^{-6}$ species (Mogica-Betancourt et al. 2014). The NiMoW/Al–Mg 10 and NiMoW/Al–Mg 15 catalyst spectra show an additional shoulder located at 320 nm that corresponds to Mo–O–Mo bridge bonds from MoO_3 in octahedral coordination (Wu et al. 2009). The presence of octahedral molybdate (MoO_3) is consistent with the XRD results. It can be observed that the intensity of the shoulders becomes smaller with the increasing addition of MgO, indicating a better dispersion of Mo species. Also, the shoulders located between 400 and 600 nm could be associated with Ni^{+2} species in tetrahedral and octahedral coordination (Yang et al. 2009). Particularly, bands in the 350–500 nm interval are generally characteristic of octahedral Ni species (Li et al. 2009). In this sense, the shoulder observed at 407 nm and the band at 490 nm corresponds to Ni^{+2} species with octahedral coordination, while the band at 594 nm is assigned to Ni^{+2} with tetrahedral coordination (Yang et al. 2009). Tetrahedral Ni^{+2} species have been associated with the formation of NiMgO or $NiAl_2O_3$ spinels, in which Ni^{+2} species strongly interact with the support and as a result, these species are more difficult to sulfide avoiding the formation of NiMoS phase (Guevara-Lara et al. 2010; Vázquez-Garrido et al. 2019) and decreasing the catalytic activity (Cervantes-Gaxiola et al. 2013). On the other hand, Ni^{+2} species in octahedral coordination are associated with Ni–Mo interactions, which facilitate the sulfidation of the species (Mogica-Betancourt et al. 2014). In general, it can be seen that as the amount of MgO increases the bands attributed to tetrahedral Ni^{+2} decreases while the bands attributed to Ni^{+2} and MoO_3 with octahedral coordination become more evident. Because of this, an improvement in catalytic activity would be expected for NiMoW/Al–Mg catalysts with an increase in MgO content up to 15 wt.%.

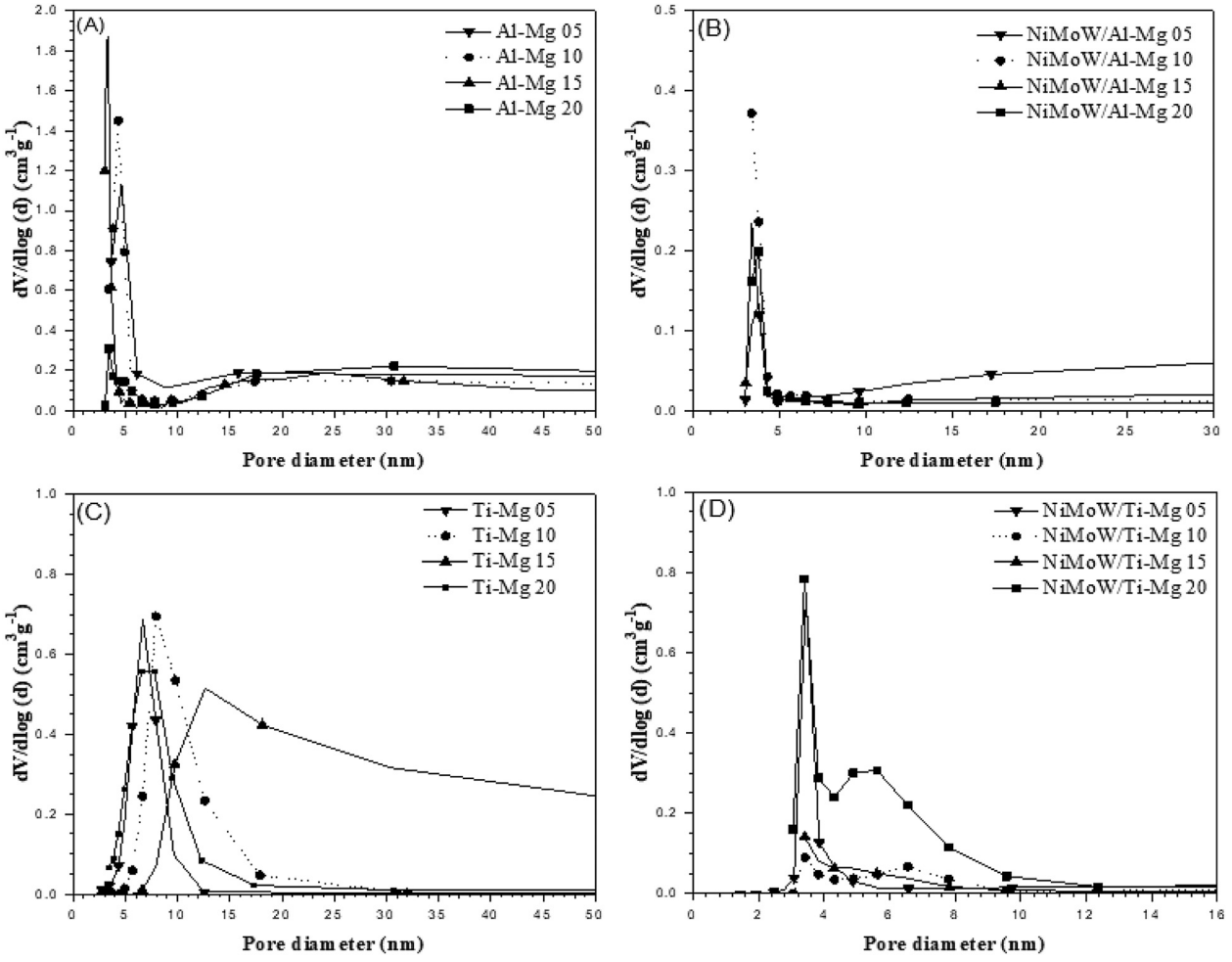

Figure 6: Pore size distribution of (A) Al–Mg mixed oxides, (B) NiMoW/Al–Mg sulfide catalysts, (C) Ti–Mg mixed oxides and (D) NiMoW/Ti–Mg sulfide catalysts.

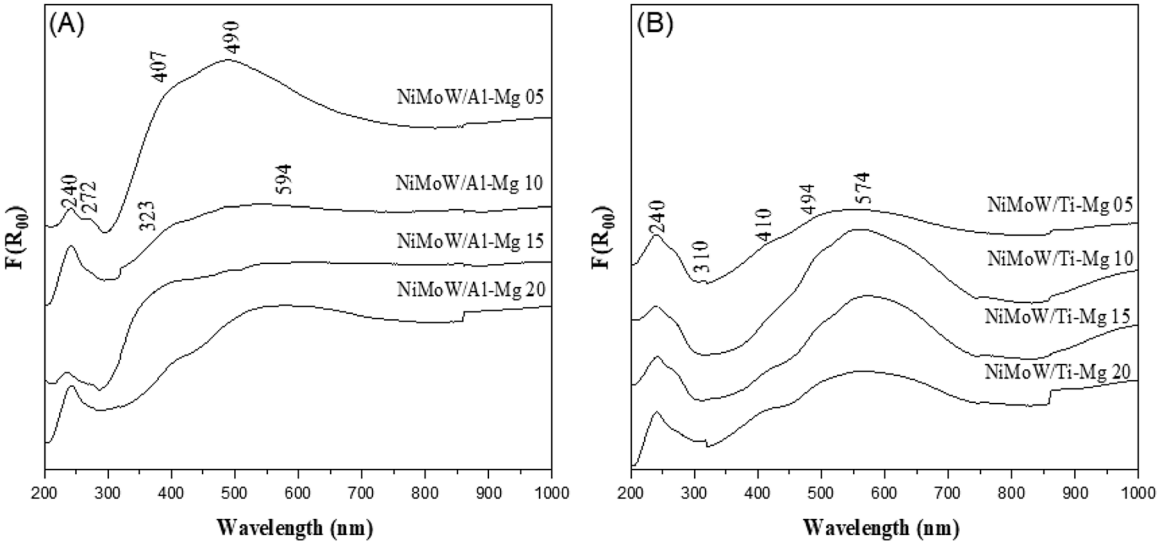

Figure 7: DRS UV–vis spectra of (A) NiMoW/Al–Mg and (B) NiMoW/Ti–Mg catalysts in the oxide state.

Table 2: % DBT conversion, the reaction rate constant and selectivity of catalysts during HDS-DBT.

Catalyst	k ($\times 10^{-7}$ mol s^{-1} g^{-1})	HYD/DDS
NiMoWS/Al–Mg 05	7.91	0.05
NiMoWS/Al–Mg 10	11.01	0.91
NiMoWS/Al–Mg 15	10.32	0.20
NiMoWS/Al–Mg 20	7.51	0.48
NiMoWS/Ti–Mg 05	8.05	0.37
NiMoWS/Ti–Mg 10	10.87	0.37
NiMoWS/Ti–Mg 15	6.60	0.26
NiMoWS/Ti–Mg 20	8.37	0.07
NiMoWS/Al–Ti 20	7.82	0.04

In addition, the UV–Vis DRS spectra of NiMoW/Ti–Mg catalysts (Figure 7B) were only analyzed in the region between 400 and 1000 nm due to the fact that bands originated from Mo and W species may be overlapped with the bands caused by $O^{-2} \rightarrow Ti^{+4}$ charge transfer of TiO_2 in the region between 200 and 400 nm (Cervantes-Gaxiola et al. 2012; Jeziorowski and Knoezinger 1979). In this sense, two shoulders at 416 nm and 494 nm are observed which can be attributed to Ni^{+2} species in octahedral coordination (Guevara-Lara et al. 2010) and the band at 574 nm is assigned to Ni^{+2} tetrahedral coordination (Cruz Pérez et al. 2016), respectively. Besides, it can be noted that the band attributed to Ni^{+2} in tetrahedral coordination is more evident with the addition of MgO, indicating a higher interaction between Ni-support on NiMoW/Ti–Mg than on NiMoW/Al–Mg catalysts.

3.5 Catalytic activity and selectivity

DBT conversion, the reaction rate constant and selectivity for all catalysts during the HDS-DBT reaction are reported in Table 2. The main products of the HDS-DBT reaction were BP and CHB, while small amounts of THDBT were also observed. Even though the metal composition was the same in all catalysts, significant differences in conversion, activity and selectivity can be observed in both series of catalysts as a function of MgO content.

Summarizing, the activity results presented in this study reveal that sulfide NiMoW/Al–Mg 10 and NiMoW/Ti–Mg 10 catalysts (68% and 64% DBT conversion, respectively) are the most active and both selective for HDS of DBT reaction being biphenyl the major product. However, the former catalyst led to a higher enhancement of the catalyst hydrogenation function which is needed for effective S-removal from refractory S-containing compounds. Besides some enhancement of the catalyst HYD function by support modification with 10 wt.% of MgO, the DDS reaction route remain as the main reaction route.

It is important to note that in both series of catalysts, the addition of 10 wt.% of MgO causes an increase in conversion. However, a further increase in MgO content provokes a decrease in catalytic activity. A similar effect was observed for NiMoWS/Al–Ti–Mg (Cervantes-Gaxiola et al. 2012) and NiMo/Mg–Al catalysts (Klimova, Solís Casados, and Ramírez 1998).

Based on the UV–vis data of the oxide precursors and XRD for sulfide catalysts, the enhanced catalyst behavior can be related to combined effects of: (i) a greater amount of octahedral species, (ii) good active phase dispersion, (iii) a higher enhancement of the catalyst hydrogenation function.

The presence of Mo and Ni with octahedral coordination at 5 and 10 wt.% of MgO observed by DRS UV–Vis could explain their performance in HDS-DBT activity. The octahedrally coordinated Mo(W) species are easily reduced. As a consequence of its easy reduction, the NiMoW/Al–Mg 10 catalyst might exhibit a larger sulfidation degree leading to better catalytic behavior in the HDS reaction (Xiong et al. 2000).

By contrast, the lower activity of the NiMoW/Ti–Mg catalysts with 15 and 20 wt.% of MgO may be related to the larger amount of Mo^{+6}(W^{+6}) ions in tetrahedral coordination, as determined by DRS UV–vis (Figure 7). Tetrahedral species are difficult to reduce or sulfide, and cannot therefore develop HDS active sites. Indeed, the direct correlation between the reducibility of the oxidic precursors and the HDS activity of the sulfided samples is widely reported in the literature (Massoth 1975; de Beer et al. 1976).

In this work, a strong influence of the support type on the phases formed is observed by XRD (Figure 3). On the one hand, the formation of large crystals of MoS_2, Ni_3S_2 and Ni_9S_8 mainly for NiMoW/Al–Mg catalysts with 15 and 20 wt.% of MgO suggests a low metal-support interaction. In addition, this behavior was showed for NiMoW/Ti–Mg catalyst with 5 wt.% of MgO. Considering that loosely bound phases are highly reducible and easily sulfided, they provide a relatively high concentration of S-vacancies in NiMoW/Al–Mg 10 catalyst (Vakros and Kordulis 2001).

The comparison of the catalytic activity for both series showed that NiMoWS/Al–Mg catalysts exhibited higher HDS-DBT activities than that observed for NiMoWS/Ti–Mg catalysts. It is important to note that most of the NiMoW/Al–Mg and NiMoW/Ti–Mg catalysts exhibited higher activities than that obtained with the NiMoWS/Al–Ti catalyst used as a reference.

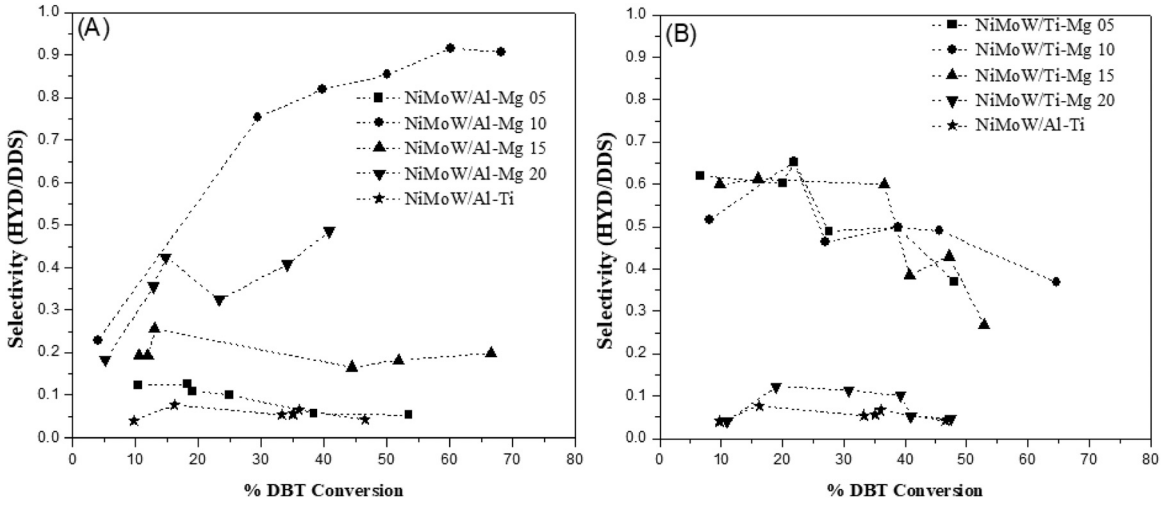

Figure 8: Selectivity as a function of DBT conversion of (A) NiMoW/Al–Mg and (B) NiMoW/Ti–Mg sulfide catalysts and the NiMoW/Al–Ti reference catalyst.

Regarding selectivity, Figure 8 shows the selectivity (HYD/DDS) as a function of DBT conversion for both series of catalysts. The results indicated that the direct DDS pathway is preferred for all catalysts; however, the addition of MgO exhibits an important effect on selectivity. It can be observed that the HYD/DDS ratio increases with the addition of MgO with a maximum for NiMoWS/Al–Mg 10 catalyst (HYD/DDS = 0.91), which exhibited the highest activity and selectivity towards the HYD pathway among all catalysts tested. Also, for the NiMoW/Al–Mg catalysts (Figure 8A) the enhancement of the HYD activity is observed with the increase in the DBT conversion. On the other hand, an opposite effect can be observed on NiMoWS/Ti–Mg catalysts (Figure 8B) where a decrease of the HYD selectivity is evident with the increase of DBT conversion.

Therefore, despite the high selectivity to the DDS pathway observed for most of the catalysts, it is possible to improve the HYD activity which is of central importance for the HDS of very heavy feedstocks by using 10 wt.% of MgO, particularly on NiMoWS/Al–Mg catalyst.

The larger hydrogenation ability of the most active catalyst can be explained assuming the "brim sites" model of the fully coordinated S-sites (Lauritsen et al. 2004a, 2004b) and taking into account that at high DBT conversion led to accumulation of a larger amount of H_2S in a batch reactor. With regard to the latter, it is well documented that the H_2S is adsorbed dissociatively on coordinatively unsaturated sites (CUS) (Echard and Leglise 2001). In such case, the inhibition of the DDS DBT transformation route might occur when H_2S formed is dissociatively adsorbed on the CUS sites leading to formation of S-saturated "brim-sites".

In conclusion, these results highlight the flexibility of the proposed catalysts in the HDS reaction since it can proceed by these two pathways adjusting the wt.% of MgO into support.

4 Conclusions

The potential of Al–Mg and Ti–Mg mixed oxides with different wt.% of MgO as viable supports for NiMoWS HDS catalysts were analyzed and compared in terms of catalytic activity with a NiMoWS/Al–Ti reference catalyst. The NiMoWS/Al–Mg catalysts exhibited more adequate properties than NiMoW/Ti–Mg; such as higher dispersion and highly reducible and easily sulfided Ni and Mo species obtaining higher catalytic activities during the HDS-DBT reaction. The effect of wt.% of MgO on NiMoWS/Al–Mg and NiMoWS/Ti–Mg catalysts in terms of catalytic activity showed a similar tendency for both series of catalysts. The results indicated that the DDS pathway is preferred for all catalysts; however, the addition of MgO exhibits an important effect on selectivity. Finally, most of the catalysts demonstrated higher catalytic activities than the reference catalysts.

Author contribution: All the authors have accepted responsibility for the entire content of this submitted manuscript and approved submission.

Research funding: Financial supports from Universidad Autónoma de Sinaloa, Dirección General de Investigación y Posgrado (DGIP), Project PROFAPI 2014/050, Projects CONACYT 182191 and CIC UMSNH 2020.

Conflict of interest statement: The authors declare no conflicts of interest regarding this article.

References

Absi-Halabi, M., A. Stanislaus, and K. Al-Dolama. 1998. "Performance Comparison of Alumina-supported Ni–Mo, Ni–W and Ni–Mo–W Catalysis in Hydrotreating Vacuum Residue." *Fuel* 77 (7): 787–90.

American Petroleum Institute (API). 2020. *Ultra Low Sulfur Diesel Fuel*. Also available at https://www.api.org/news-policy-and-issues/fuels-and-renewable-policy/us-fuel-requirements/ultra-low-sulfur-diesel-fuel.

Ansari, A., A. Ali, M. Asif, and S. Uzzaman. 2017. "Microwave-assisted MgO NP Catalyzed One-Pot Multicomponent Synthesis of Polysubstituted Steroidal Pyridines." *New Journal of Chemistry*. 42, 184–197.

Caloch, B., M. S. Rana, and J. Ancheyta. 2004. "Improved Hydrogenolysis (C–S, C–M) Function With Basic Supported Hydrodesulfurization Catalysts." *Catalysis Today* 98 (1): 91–8.

Candia, R., B. S. Clausen, and H. Topsøe. 1982. "The Origin of Catalytic Synergy in Unsupported Co-Mo HDS Catalysts." *Journal of Catalysis* 77 (2): 564–6.

Cervantes-Gaxiola, M. E., M. Arroyo-Albiter, R. Maya-Yescas, J. L. Rico-Cerda, A. Guevara-Lara, and J. Espino-Valencia. 2012. "Synthesis, Characterization and Catalytic Activity During Hydrodesulphurization of Dibenzothiophene of NiMoW Catalysts Supported on Al-Ti Mixed Oxides Modified With MgO." *Fuel* 100: 57–65.

Cervantes-Gaxiola, M. E., M. Arroyo-Albiter, A. Pérez-Larios, P. B. Balbuena, and J. Espino-Valencia. 2013. "Experimental and Theoretical Study of NiMoW, NiMo, and NiW Sulfide Catalysts Supported on an AlTiMg Mixed Oxide During the Hydrodesulfurization of Dibenzothiophene." *Fuel* 113: 733–43.

Chianelli, R. R., and G. Berhault. 1999. "Symmetrical Synergism and the Role of Carbon in Transition Metal Sulfide Catalytic Materials." *Catalysis Today* 53 (3): 357–66.

Chianelli, R. R., A. F. Ruppert, M. José-Yacamán, and A. Vázquez-Zavala. 1995. "HREM Studies of Layered Transition Metal Sulfide Catalytic Materials." *Catalysis Today* 23 (3): 269–81.

Chianelli, R. R., G. Berhault, P. Raybaud, S. Kasztelan, J. Hafner, and H. Toulhoat. 2002. "Periodic Trends in Hydrodesulfurization: In support of the Sabatier Principle." *Applied Catalysis A: General* 227 (1): 83–96.

Costa, P. D., C. Potvin, J.-M. Manoli, B. Genin, and G. Djéga-Mariadassou. 2004. "Deep Hydrodesulphurization and Hydrogenation of Diesel Fuels on Alumina-supported and Bulk Molybdenum Carbide Catalysts." *Fuel* 83 (13): 1717–26.

Cruz-Perez, A. E., A. Guevara-Lara, J. P. Morales-Ceron, A. Alvarez-Hernandez, J. A. de Reyes, L. Massin, C. Geantet, and M. Vrinat. 2011. "Ni and W Interactions in the Oxide and Sulfide States on an Al_2O_3–TiO_2 Support and Their Effects on Dibenzothiophene Hydrodesulfurization." *Catalysis Today* 172 (1): 203–8.

Cruz-Pérez, A. E., Y. Torrez Jiménez, J. J. Velasco Alejo, T. A. Zepeda, D. M. Frías Márquez, M. G. Rivera Ruedas, S. Fuentes, and J. N. Díaz de León. 2016. "NiW/MgO–TiO_2 Catalysts for Dibenzothiophene Hydrodesulfurization: Effect of Preparation Method." *Catalysis Today* 271: 28–34.

de Beer, V. H. J., C. Bevelander, T. H. M. van Sint Fiet, P. G. A. J. Werter, and C. H Amberg. 1976. "The CoO-MoO_3-γ-Al_2O_3 Catalyst: VI. Sulfur Content Analysis and Hydrodesulfurization Activities." *Journal of Catalysis* 43 (1): 68–77.

Díaz de León, J. N., C. Ramesh Kumar, J. Antúnez-García, and S. Fuentes-Moyado. 2019. "Recent Insights in Transition Metal Sulfide Hydrodesulfurization Catalysts for the Production of Ultra Low Sulfur Diesel: A Short Review." *Catalysts* 9 (1): 87.

Dik, P. P., V. Y. Pereima, K. A. Nadeina, M. O. Kazakov, O. V. Klimov, E. Y. Gerasimov, I. P. Prosvirin, and A. S. Noskov. 2018. "Hydrocracking of Vacuum Gasoil on NiMoW/AAS-Al_2O_3 Trimetallic Catalysts: Effect of the W : Mo Ratio." *Catalysis in Industry* 10 (1): 20–8.

Duan, A., G. Wan, Z. Zhao, C. Xu, Y. Zheng, Y. Zhang, T. Dou, X. Bao, and K. Chung. 2007. "Characterization and Activity of Mo Supported Catalysts for Diesel Deep Hydrodesulphurization." *Catalysis Today* 119 (1): 13–8.

Dufresne, P., N. Brahma, F. Labruyère, M. Lacroix, and M. Breysse. 1996. "Activation of Off Site Presulfided Cobalt-Molybdenum Catalysts." *Catalysis Today* 29 (1): 251–4.

Echard, M., and J. Leglise. 2001. "Sulphidation of an Oxidic CoMo/Al_2O_3 Catalyst Under Practical Conditions: Different Kinds of Sulphur Species." *Catalysis Letters* 72 (1): 83–9.

El-Sayed, S. M., M. A. Amer, T. M. Meaz, N. M. Deghiedy, and H. A. El-Shershaby. 2018. "Investigational Analysis on Irradiated MgO–TiO_2 Binary Oxide." *Materials Research Express* 5 (5): 56508.

Girgis, M. J., and B. C. Gates. 1991. "Reactivities, Reaction Networks, and Kinetics in High-pressure Catalytic Hydroprocessing." *Industrial & Engineering Chemistry* Research 30 (9): 2021–58.

Göbölös, S., Q. Wu, O. André, F. Delannay, and B. Delmon. 1986. "Correlation Between Hydrodesulphurization Activity and Reducibility of Unsupported MoS_2-Based Catalysts Promoted by Group VIII Metals." *Journal of the Chemical Society, Faraday Transactions 1: Physical Chemistry in Condensed Phases* 82 (8): 2423–34.

Gómez-Orozco, S. Y., R. Huirache-Acuña, B. Pawelec, J. L. G. Fierro, E. M. Rivera-Muñoz, J. Lara-Romero, and G. Alonso-Nuñez. 2018. "Characterizations and HDS Performances of Sulfided NiMoW Catalysts Supported on Mesoporous Titania-modified SBA-15." *Catalysis Today* 305: 152–61.

González-Cortés, S. L., S. Rugmini, T. Xiao, M. L. H. Green, S. M. Rodulfo-Baechler, and F. E. Imbert. 2014. "Deep Hydrotreating of Different Feedstocks Over a Highly Active Al_2O_3-Supported NiMoW Sulfide Catalyst." *Applied Catalysis A: General* 475: 270–81.

Grzechowiak, J. R., J. Rynkowski, and I Wereszczako-Zieliñska. 2001. "Catalytic Hydrotreatment on Alumina–Titania supported NiMo Sulphides." *Catalysis Today* 65 (2): 225–31.

Guevara-Lara, A., A. E. Cruz-Pérez, Z. Contreras-Valdez, J. Mogica-Betancourt, A. Alvarez-Hernández, and M. Vrinat. 2010. "Effect of Ni Promoter in the Oxide Precursors of MoS_2/MgO–Al_2O_3 Catalysts Tested in Dibenzothiophene Hydrodesulphurization." *Catalysis Today* 149 (3): 288–94.

Guzmán, M. A., R. Huirache-Acuña, C. V. Loricera, J. R. Hernández, J. N. Díaz de León, J. A. de los Reyes, and B. Pawelec. 2013. "Removal of Refractory S-containing Compounds from Liquid Fuels Over P-loaded NiMoW/SBA-16 Sulfide Catalysts." *Fuel* 103: 321–33.

Harris, S., and R. R. Chianelli. 1984. "Catalysis by Transition Metal Sulfides: The Relation Between Calculated Electronic Trends and HDS Activity." *Journal of Catalysis* 86 (2): 400–12.

Houalla, M., D. H. Broderick, A. V. Sapre, N. K. Nag, V. H. J. de Beer, B. C. Gates, and H. Kwart. 1980. "Hydrodesulfurization of Methyl-substituted Dibenzothiophenes Catalyzed by Sulfided Co-Moγ-Al_2O_3." *Journal of Catalysis* 61 (2): 523–7.

Huang, Z. D., W. Bensch, L. Kienle, S. Fuentes, G. Alonso, and C. Ornelas. 2008. "Preparation and Characterization of SBA-15 Supported Cobalt–Molybdenum Sulfide Catalysts for HDS Reaction: An All Sulfide Route to Hydrodesulfurization Catalysts." *Catalysis Letters* 124 (1): 24.

Huirache-Acuña, R., M. A. Albiter, C. Ornelas, F. Paraguay-Delgado, R. Martínez-Sánchez, and G. Alonso-Nuñez. 2006. "Ni(Co)-Mo-W Sulphide Unsupported HDS Catalysts by Ex Situ Decomposition of Alkylthiomolybdotungstates." *Applied Catalysis A: General* 308: 134–42.

Huirache-Acuña, R., B. Pawelec, C. V. Loricera, E. M. Rivera-Muñoz, R. Nava, B. Torres, and J. L. Fierro. 2012. "Comparison of the Morphology and HDS Activity of Ternary Ni(Co)-Mo-W Catalysts Supported on Al-HMS and Al-SBA-16 Substrates." *Applied Catalysis B: Environmental* 125: 473–85.

Jeziorowski, H., and H. Knoezinger. 1979. "Raman and Ultraviolet Spectroscopic Characterization of Molybdena on Alumina Catalysts." *The Journal of Physical Chemistry* 83 (9): 1166–73.

Kelty, S. P., G. Berhault, and R. R. Chianelli. 2007. "The Role of Carbon in Catalytically Stabilized Transition Metal Sulfides." *Applied Catalysis A: General* 322: 9–15.

Klicpera, T., and M. Zdražil. 1999. "High Surface Area MoO_3/MgO: Preparation by the New Slurry Impregnation Method and Activity in Sulphided State in Hydrodesulphurization of Benzothiophene." *Catalysis Letters* 58 (1): 47–51.

Klicpera, T., and M. Zdražil. 2002. "Preparation of High-Activity MgO-supported Co–Mo and Ni–Mo Sulfide Hydrodesulfurization Catalysts." *Journal of Catalysis* 206 (2): 314–20.

Klimova, T., D. Solís Casados, and J. Ramírez. 1998. "New Selective Mo and NiMo HDS Catalysts Supported on Al_2O_3–MgO(x) Mixed Oxides." *Catalysis Today* 43 (1): 135–46.

Knudsen, K. G., B. H. Cooper, and H. Topsøe. 1999. "Catalyst and Process Technologies for Ultra Low Sulfur Diesel." *Applied Catalysis A: General* 189 (2): 205–15.

Krüss, G. 1884. "Ueber die Schwefelverbindungen des Molybdäns." *Justus Liebigs Annalen der Chemie* 225 (1): 1–57.

Lan, L., S. Ge, K. Liu, Y. Hou, and X. Bao. 2011. "Synthesis of Ni_2P Promoted Trimetallic NiMoW/γ-Al_2O_3 Catalysts for Diesel Oil Hy drotreatment." *Journal of Natural Gas Chemistry* 20 (2): 117–22.

Lauritsen, J. V., M. V. Bollinger, E. Lægsgaard, K. W. Jacobsen, J. K. Nørskov, B. S. Clausen, H. Topsøe, and F. Besenbacher. 2004a. "Atomic-scale Insight into Structure and Morphology Changes of MoS_2 Nanoclusters in Hydrotreating Catalysts." *Journal of Catalysis* 221 (2): 510–22.

Lauritsen, J. V., M. Nyberg, J. K. Nørskov, B. S. Clausen, H. Topsøe, E. Lægsgaard, and F. Besenbacher. 2004b. "Hydrodesulfurization Reaction Pathways on MoS_2 Nanoclusters Revealed by Scanning Tunneling Microscopy." *Journal of Catalysis* 224 (1): 94–106.

Leyva, C., J. Ancheyta, A. Travert, F. Maugé, L. Mariey, J. Ramírez, and M. S. Rana. 2012. "Activity and Surface Properties of NiMo/SiO_2–Al_2O_3 Catalysts for Hydroprocessing of Heavy Oils." *Applied Catalysis A: General* 425-426: 1–12.

Li, X., F. Zhou, A. Wang, L. Wang, and Y. Hu. 2009. "Influence of Templates on the Overgrowth of MCM-41 over HY and the Hydrodesulfurization Performances of the Supported Ni–Mo Catalysts." *Industrial & Engineering Chemistry Research* 48 (6): 2870–7.

Massoth, F. E. 1975. "Studies of Molybdena-Alumina Catalysts: IV. Rates and Stoichiometry of Sulfidation." *Journal of Catalysis* 36 (2): 164–84.

Mendoza-Nieto, J. A., O. Vera-Vallejo, L. Escobar-Alarcón, D. Solís-Casados, and T. Klimova. 2013. "Development of New Trimetallic NiMoW Catalysts Supported on SBA-15 for Deep Hydrodesulfurization." *Fuel* 110: 268–77.

Mendoza-Nieto, J. A., A. Vizueth-Montes de Oca, L. A. Calzada, and T. E. Klimova. 2019. "Trimetallic NiMoW and CoMoW Catalysts Supported on SBA-15 Modified With Titania or Zirconia for Deep Hydrodesulfurization." *Catalysis Today*, https://doi.org/10.1016/j.cattod.2019.06.023.

Mogica-Betancourt, J. C., A. López-Benítez, J. R. Montiel-López, L. Massin, M. Aouine, M. Vrinat, G. Berhault, and A. Guevara-Lara. 2014. "Interaction Effects of Nickel Polyoxotungstate with the Al_2O_3–MgO Support for Application in Dibenzothiophene Hydrodesulfurization." *Journal of Catalysis* 313: 9–23.

Mozhaev, A. V., M. S. Nikul'shina, C. Lancelot, P. Blanchard, C. Lamonier, and P. A. Nikul'shin. 2018. "Trimetallic Hydrotreating Catalysts CoMoW/Al_2O_3 and NiMoW/Al_2O_3 Prepared on the Basis of Mixed Mo-W Heteropolyacid: Difference in Synergistic Efects." *Petroleum Chemistry* 58 (14): 1198–205.

Nava, H., F. Pedraza, and G. Alonso. 2005. "Nickel-Molybdenum-Tungsten Sulfide Catalysts Prepared by In Situ Activation of Trimetallic (Ni-Mo-W) Alkylthiomolybdotungstates." *Catalysis Letters* 99 (1): 65–71.

Nikulshina, M. S., A. V. Mozhaev, P. P. Minaev, M. Fournier, C. Lancelot, P. Blanchard, E. Payen, C. Lamonier, and P. A. Nikulshin. 2017. "Trimetallic NiMoW/Al_2O_3 Hydrotreating Catalyst Based on $H_4SiMo_3W_9O_{40}$ Mixed Heteropoly Acid." *Russian Journal of Applied Chemistry* 90 (7): 1122–9.

Okamoto, Y., M. Breysse, G. Murali Dhar, and C. Song. 2003. "Effect of Support in Hydrotreating Catalysis for Ultra Clean Fuels." *Catalysis Today* 86 (1): 1–3.

Okamoto, Y. 2014. "Novel Molecular Approaches to the Structure-Activity Relationships and Unique Characterizations of Co–Mo Sulfide Hydrodesulfurization Catalysts for the Production of Ultraclean Fuels." *Bulletin of the Chemical Society of Japan* 87 (1): 20–58.

Portela, L., P. Grange, and B. Delmon. 1995. "XPS and NO Adsorption Studies on Alumina-Supported Co-Mo Catalysts Sulfided by Different Procedures." *Journal of Catalysis* 156 (2): 243–54.

Priecel, P., D. Kubicka, L. Capek, Z. Bastl, and P. Rysanek. 2011. "The Role of Ni Species in the Deoxygenation of Rapeseed Oil over NiMo-Alumina Catalysts." *Applied Catalysis A: General* 397 (1-2): 127–37.

Ramanathan, K., and S. W. Weller. 1985. "Characterization of Tungsten Sulfide Catalysts." *Journal of Catalysis* 95 (1): 249–59.

Ramírez, J., and A. D. Gutiérrez-Alejandre. 1998. "Relationship Between Hydrodesulfurization Activity and Morphological and Structural Changes in NiW Hydrotreating Catalysts Supported on Al_2O_3–TiO_2 Mixed Oxides." *Catalysis Today* 43 (1): 123–33.

Rana, M. S., M. L. Huidobro, J. Ancheyta, and M. T. Gómez. 2005. "Effect of Support Composition on Hydrogenolysis of Thiophene and Maya Crude." *Catalysis Today* 107–108: 346–54.

Rana, M. S., A. Al-Barood, R. Brouresli, A. W. Al-Hendi, and N. Mustafa. 2018. "Effect of Organic Nitrogen Compounds on Deep Hydrodesulfurization of Middle Distillate." *Fuel Processing Technology* 177: 170–8.

Ríos-Caloch, G., V. Santes, J. Escobar, P. Pérez-Romo, L. Díaz, and L. Lartundo-Rojas. 2016. "Effect of Chitosan on the

Performance of NiMoP-Supported Catalysts for the Hydrodesulfurization of Dibenzothiophene." *Journal of Nanomaterials* 2016: 4047874.

Romero-Toledo, R., M. Bravo-Sánchez, G. Rangel-Porras, R. Fuentes-Ramírez, A. Pérez-Laríos, A. Medina-Ramirez, M. Martínez-Rosales. 2018. "Effect of Mg as Impurity on the Structure of Mesoporous γ-Al_20_3: Efficiency as Catalytic Support in HDS of DBT." *International Journal of Chemical Reactor Engineering* 16 (11): 1–16.

Sajjadi, S. M., M. Haghighi, and F. Rahmani. 2015. "Sol–gel Synthesis of Ni–Co/Al_2O_3–MgO–ZrO_2 Nanocatalyst Used in Hydrogen Production via Reforming of CH_4/CO_2 Greenhouse Gases." *Journal of Natural Gas Science and Engineering* 22: 9–21.

Scheffer, B., N. J. J. Dekker, P. J. Mangnus, and J. A. Moulijn. 1990. "A Temperature-programmed Reduction Study of Sulfided Co-Mo/Al_2O_3 Hydrodesulfurization Catalysts." *Journal of Catalysis* 121 (1): 31–46.

Sigurdson, S., V. Sundaramurthy, A. K. Dalai, and J. Adjaye. 2008. "Phosphorus Promoted Trimetallic NiMoW/γ–Al_2O_3 Sulfide Catalysts in Gas Oil Hydrotreating." *Journal of Molecular Catalysis A: Chemical* 291 (1): 30–7.

Soled, S. L., S. Miseo, R. Krycak, H. Vroman, T. C. Ho, and K. L. Riley. 2001. *Nickel Molybodtungstate Hydrotreating Catalysts* (*law444*). US Patent 6 (299). 760B761.

Solis, D., T. Klimova, J. Ramírez, and T. Cortez. 2004. "NiMo/Al_2O_3–MgO (x) Catalysts: The Effect of the Prolonged Exposure to Ambient Air on the Textural and Catalytic Properties." *Catalysis Today* 98 (1): 99–108.

Solís-Casados, D. A., L. Escobar-Alarcón, T. Klimova, J. Escobar-Aguilar, E. Rodríguez-Castellón, J. A. Cecilia, C. Morales-Ramírez. 2016. "Catalytic performance of CoMo/Al_2O_3-MgO-Li(x) formulations in DBT hydrodesulfurization." *Catalysis Today* 271, 35–44.

Solís-Casados, D. A., C. E. Rodríguez-Nava, T. Klimova, L. Escobar-Aguilar. 2019. "Selective HDS of DBT using a K_2O-modified CoMoW/Al_2O_3-MgO catalytic formulation." *Catalysis Today* 271, 35–44. In press.

Topsøe, H., and B. S. Clausen. 1984. "Importance of Co-Mo-S Type Structures in Hydrodesulfurization." *Catalysis Reviews* 26 (3-4): 395–420.

Topsøe, H. 2007. "The Role of Co–Mo–S Type Structures in Hydrotreating Catalysts." *Applied Catalysis A: General* 322: 3–8.

Trejo, F., M. S. Rana, and J. Ancheyta. 2008. "CoMo/MgO–Al_2O_3 Supported Catalysts: An Alternative Approach to Prepare HDS Catalysts." *Catalysis Today* 130 (2): 327–36.

U.S. Enviromental Protection Agency. 2006. *Diesel Fuel Standards*. Also available at https://www.epa.gov/diesel-fuel-standards.

Vakros, J., and C. Kordulis. 2001. "On the Synergy Between Tungsten and Molybdenum in the W-incorporated CoMo/γ-Al_2O_3 Hydrodesulfurization Catalysts." *Applied Catalysis A: General* 217 (1): 287–93.

van Haandel, L., M. Bremmer, P. J. Kooyman, J. A. R. van Veen, T. Weber, and E. J. M. Hensen. 2015. "Structure–Activity Correlations in Hydrodesulfurization Reactions over Ni-Promoted $Mo_xW_{(1-x)}S_2/Al_2O_3$ Catalysts." *ACS Catalysis* 5 (12): 7276–87.

Vangestel, J., J. Leglise, and J. C. Duchet. 1994. "Catalytic Properties of a Como/Al_2O_3 Catalyst Presulfided with Alkyl Polysulfides: Comparison with Conventional Sulfiding." *Journal of Catalysis* 145 (2): 429–36.

Vázquez-Garrido, I., A. López-Benítez, G. Berhault, and A. Guevara-Lara. 2019. "Effect of Support on the Acidity of NiMo/Al_2O_3-MgO and NiMo/TiO_2–Al_2O_3 Catalysts and on the Resulting Competitive Hydrodesulfurization/Hydrodenitrogenation Reactions." *Fuel* 236: 55–64.

Vázquez-Salas, P. J., R. Huirache-Acuña, T. A. Zepeda, G. Alonso-Núñez, R. Maya-Yescas, N. Mota, and B. Pawelec. 2018. "Enhancement of Dibenzothiophene Hydrodesulphurization via Hydrogenation Route on NiMoW Catalyst Supported on HMS Modified with Ti." *Catalysis Today* 305: 65–74.

Vega-Granados, K., M. Del Valle, A. Licea-Claverie, G. Alonso-Núñez, R. Romero-Rivera, L. López-Sosa, M. Avalos-Borja, and J. Cruz-Reyes. 2017. "A New Route for the Synthesis of Ammonium Thiotungstate, a Catalyst Precursor." *Catalysis Letters* 147 (6): 1339–46.

Vrinat, M., M. Breysse, C. Geantet, J. Ramirez, and F. Massoth. 1994. "Effect of MoS_2 Morphology on the HDS Activity of Hydrotreating Catalysts." *Catalysis Letters* 26 (1): 25–35.

Wu, L., D. Jiao, J.-A. Wang, L. Chen, and F. Cao. 2009. "The Role of MgO in the Formation of Surface Active Phases of CoMo/Al_2O_3–MgO Catalysts for Hydrodesulfurization of Dibenzothiophene." *Catalysis Communications* 11 (4): 302–5.

Xiong, G., Z. Feng, J. Li, Q. Yang, P. Ying, Q. Xin, and C. Li. 2000. "UV Resonance Raman Spectroscopic Studies on the Genesis of Highly Dispersed Surface Molybdate Species on γ-Alumina." *The Journal of Physical Chemistry B* 104 (15): 3581–8.

Yang, R., X. Li, J. Wu, X. Zhang, and Z. Zhang. 2009. "Promotion Effects of Copper and Lanthanum Oxides on Nickel/Gamma-Alumina Catalyst in the Hydrotreating of Crude 2-Ethylhexanol." *Journal of Physical Chemistry C* 113 (41): 17787–94.